

Programming sites of meiotic crossovers using Spo11 fusion proteins

Roberta Sarno^{1,2}, Yoan Vicq^{1,2}, Norio Uematsu^{1,2}, Marine Luka^{1,2}, Clement Lapierre^{1,2}, Dana Carroll³, Giacomo Bastianelli⁴, Alexandre Serero^{1,2,*} and Alain Nicolas^{1,2,*}

¹Institut Curie, PSL Research University, CNRS UMR3244, Recombination and Genetic Instability, Paris F-75005, France, ²Sorbonne Universités, UPMC Université Paris 06, CNRS UMR3244, Paris F-75005, France, ³Department of Biochemistry, University of Utah School of Medicine, Salt Lake City, UT 84112-5650, USA and ⁴Meiogenix, Paris F-75012, France

Received May 30, 2017; Revised August 03, 2017; Editorial Decision August 10, 2017; Accepted August 17, 2017

ABSTRACT

Meiotic recombination shapes the genetic diversity transmitted upon sexual reproduction. However, its non-random distribution along the chromosomes constrains the landscape of potential genetic combinations. For a variety of purposes, it is desirable to expand the natural repertoire by changing the distribution of crossovers in a wide range of eukaryotes. Toward this end, we report the local stimulation of meiotic recombination at a number of chromosomal sites by tethering the natural Spo11 protein to various DNA-binding modules: full-length DNA binding proteins, zinc fingers (ZFs), transcription activator-like effector (TALE) modules, and the CRISPR-Cas9 system. In the yeast *Saccharomyces cerevisiae*, each strategy is able to stimulate crossover frequencies in naturally recombination-cold regions. The binding and cleavage efficiency of the targeting Spo11 fusions (TSF) are variable, being dependent on the chromosomal regions and potential competition with endogenous factors. TSF-mediated genome interrogation distinguishes naturally recombination-cold regions that are flexible and can be warmed-up (gene promoters and coding sequences), from those that remain refractory (gene terminators and centromeres). These results describe new generic experimental strategies to increase the genetic diversity of gametes, which should prove useful in plant breeding and other applications.

INTRODUCTION

In eukaryotes, meiotic recombination between the homologous chromosomes disrupts the physical linkage between

the parental alleles, generating the haplotype diversity transmitted to the offspring by the gametes. Recombination also helps homologous chromosome to pair and their physical connection by the crossover molecules, ensures accurate chromosome segregation during the first of the two meiotic divisions. The absence or the mis-localization of the crossovers is a source of sterility (1).

Meiotic recombination is neither randomly nor homogeneously distributed along the chromosomes, as reflected by the large distortion observed between the genetic and physical distances along the chromosomes as well as by the large variation in average recombination frequencies between species. Recombination is initiated by the evolutionarily conserved Spo11 protein, that generates DNA double-strand breaks (2,3), which are subsequently repaired on the homologous chromosomes to yield the non-crossover (gene conversion) and crossover molecules (CO) (4). In the yeast *Saccharomyces cerevisiae*, ~160–200 DSBs form per cell and the majority leads to recombination events (5,6). In contrast, in *Arabidopsis thaliana* there are ~200–300 DSBs per cell but only ~10 crossovers occur per meiosis (7). Similarly, there are ~200–300 DSBs per cell in mouse and only ~24 crossovers per meiosis (8). Clearly, in every species, DSBs are more likely to occur in some genomic regions than in others, being related to the Spo11 chromatin association and cleavage probabilities varying by several order of magnitude from site to site but also due to the combinatorial action of several factors acting at different scales (5), including crossover homeostasis (9) and feedback mechanisms controlling DSB formation (10–12). Extreme is the regional distribution of crossovers towards the distal regions in barley and wheat crop species (13). For example, in the wheat chromosome 3B (~1 Gb long), crossovers are clustered in only 13% of the chromosome (14). Thus, the highly skewed distribution of meiotic recombination generates large non-recombining regions and limits the ability to associate or

*To whom correspondence should be addressed. Tel: +33 1 56 24 65 20; Fax: +33 1 56 24 66 44; Email: alain.nicolas@curie.fr
Correspondence may also be addressed to Alexandre Serero. Email: alexandre.serero@curie.fr
Present address: Norio Uematsu, Shiodome Building, 1-2-20 Kalgan, Minato-Ku, Tokyo 105-0022, Japan.

separate genes over a small number of generations. To overcome such limit, the development of methods to program the frequency and localization of meiotic recombination remains to be achieved.

Mechanistically, meiotic recombination initiation is a ubiquitous and tightly regulated multi-step process, closely integrated with the development of meiosis-specific higher order chromosome structures (4,11,15–17). An important common determinant of DSB formation is the accessibility of the chromatin to the recombination machinery. Chromatin accessibility related to low nucleosome occupancy contributes to the bias that favours DSB formation and/or recombination in promoter regions as observed in yeasts (5,18) and *A. thaliana* (7). Nevertheless, not all nucleosome depleted regions are sites of DSB formation. Intriguingly, in contrast to the rapidly evolving PRDM9-dependent hotspots in mammals (19), recent studies in distant species of budding yeast (18) and birds (20) revealed that most hotspots are evolutionarily conserved, suggesting that strong mechanistic and/or evolutionary constraints play a role in designating the preferred DSB sites. In addition, the resolution of the recombination intermediates into gene conversion or crossover products is tightly controlled, limiting the number but ensuring at least one crossover per homolog.

Together, the complexity of the recombination process and its mechanistic and regulatory constraints suggested that it may be difficult to modify meiotic recombination frequencies and sites without inducing sterility. However, and perhaps paradoxically, meiotic recombination seems to remain flexible (17,21–24). Earlier experiments showed that, in yeast, fusion of Spo11 to the Gal4 DNA-binding domain (Gal4BD) was sufficient to induce DSB formation and recombination at Gal4 binding sites (Gal4_{UAS}) in naturally cold regions (21,25,26). This Spo11-tethering strategy remains limited, being constrained to targeting endogenous Gal4_{UAS} sites. In addition, many of these sites are not bound by the Gal4BD-Spo11 protein *in vivo* or are bound but remain refractory to DSB formation (26). In *A. thaliana*, where the total number of DSBs per cell greatly exceeds the number of crossovers, mutations or increased dosage of recombination modifiers (FANCM, FIGL1, RECQ4, HEI10) have led to an increase in recombination (27–30). However, these methods elevate crossover numbers solely in naturally initiating regions and does not allow to modify DSB refractory regions. Thus, to induce crossovers throughout the genome, it remains necessary to develop methods allowing to direct DSBs to arbitrarily chosen sites.

Here, we report the development of a series of targeting Spo11 fusions (TSFs), carrying a variety of DNA binding modules that allowed us to vary the location and/or the number of recombination initiation sites. Our results define a versatile and customizable Spo11-based platform to interrogate naturally DSB-cold regions and to target meiotic recombination in eukaryotic cells, highlighting its generic potential for biotechnological applications.

MATERIALS AND METHODS

Plasmid constructions

The plasmids used in this work are listed in Supplementary Table S1. All plasmids are derivatives of pAP1 and pAP11 (21,25) which contain the *GAL4BD-SPO11* fusion gene flanked by the *ADHI* promoter and transcription terminator. To exchange the *GAL4BD* region with other Spo11-targeting modules, the desired *in vitro*-built PCR fragment flanked by a *SpeI* and an *XmaI* site was introduced between the *ADHI* promoter and the *XmaI* site located within the 36 nt internal linker (PEFMAMEAPGIR) that separates the targeting module and the N-terminal region of the full-length *S. cerevisiae* Spo11 coding region. Sequences encoding the full-length proteins Gal4 (560 aa), Tec1 (486 aa), Rsc3 (885 aa) and Mtw1 (290 aa) were amplified by PCR from the wild type SK1 yeast strain ORD7254–25D. The pRSM046, pRSM026, pRSM070 and pMLM023 plasmids contain the *GAL4-SPO11*, *TEC1-SPO11*, *RSC3-SPO11* and *MTW1-SPO11* fusions, respectively. To build the *QQR-SPO11* gene construct, the *QQR* coding fragment (encoding 101 aa) was PCR-amplified from the *QQR*-pET15b plasmid (31) and cloned into the pAP11 plasmid to yield pAP119 plasmid. Regarding the *dCAS9-SPO11* gene construct we first designed the sequence of a yeast codon-optimized version of the Cas9 protein from *Streptococcus pyogenes* (1368 aa) and containing inactivating D10A and H840A mutations (dCas9) (32). A nuclear localization signal (NLS, GGMAAPKKRKYVDGG) was attached to the N-terminus of dCas9 to promote nuclear import. The NLS and N-terminus of the dCas9 protein were separated by an internal linker (GIHGVPAA) (33). The *NLS-dCAS9* construct was synthesized by GenScript and cloned into a pUC57 vector to create pScdCas9. The pRSM026 *SpeI-XmaI* fragment was replaced by the *SpeI-XmaI* fragment from pScdCas9 plasmid to yield the pAS502 plasmid. To attach the 6xHis-3xFlag tag to the C-terminus of the Spo11 protein, the 6xHis-3xFlag coding sequence was PCR amplified from ANT2152 (*SPO11-6xHis-3xFlag-KanMX*) and Gibson assembled into the *NdeI*-linearized pAS502 plasmid by using the NEB Gibson Assembly kit. The resulting pAS504 plasmid contains the *P_{ADHI}-NLS-dCAS9-SPO11-6xHis-3xFlag-T_{ADHI}* construct. The dCas9-Spo11 and dCas9-Spo11-6xHis-3xFlag constructs display very similar capacities to complement *spo11Δ* sporulation defects and to induce meiotic DSB formation. The TALE array (encoding 1097 aa) was synthesized by GeneArt (Life Technologies™) and provided in the pDONR221 vector. The NLS-TALE fragment was cloned into a *SpeI/XmaI*-digested pRSM046 plasmid to obtain pMLM060. The DNA sequence of the seven TSF constructs is reported in the Supplementary Material (Figure S1).

The guide RNA (gRNA) expression plasmids were constructed from the *P_{RPRI}-gRNA_handle.T_{RPRI}* plasmid (34) which was a gift from Timothy Lu (Addgene plasmid #49014). This plasmid, called thereafter p_gRNA_handle, encodes the gRNA backbone (without the guide sequence) whose expression is driven by the constitutive *RPRI* promoter (an RNA-polymerase-III-dependent promoter). For the synthesis and cloning of each guide se-

quence into p_gRNA_handle, two complementary oligonucleotides, each carrying the 20-nt guide sequence, were designed. Both oligonucleotides also bear at the 5' end a 40-nt sequence identical to the regions flanking the *HindIII* site of p_gRNA_handle. We used this pair of oligonucleotides to PCR amplify the 100-bp fragment and then cloned it into the *HindIII* site of the p_gRNA_handle vector by one-step Gibson assembly. Oligonucleotides used to construct each guide sequence are listed in Supplementary Table S2. To construct a multiplex gRNAs expression vector a multiple cloning sites sequence providing eight unique cloning sites (*ApaI*, *NcoI*, *NdeI*, *PstI*, *SmaI*, *SphI*, *BamHI* and *BglII*) was introduced into the *SacI* site of the p_gRNA_handle vector by one-step Gibson assembly, to yield the pAS08 plasmid. Multiple gRNA expression cassettes, each containing the *RPR1* promoter, a gRNA sequence and the *RPR1* terminator, were PCR amplified from the corresponding single gRNA expression plasmid and Gibson assembled into the *NcoI* site of the pAS08 plasmid. All plasmid constructs were verified by restriction digestion and Sanger sequencing.

Yeast strains

The genotypes of the diploid *S. cerevisiae* strains used in this work are listed in Supplementary Table S1. They are derivatives of SK1 (35) and were obtained by one-step transformation of haploid parents or recovered from genetic crosses. All strains, except ORD7304 (gift of V. Borde) and ORD8175 (25) were constructed for this work. For introduction into the yeast genome, all TSF expression plasmids except pAP119 plasmid, were linearized by digestion with *XbaI*. pAP119 plasmid was digested by *Bsu36I*. Linearized TSF plasmids were integrated at the *TRP1* locus by transformation of the strain AND1940-4D (*MAT* α , *spo11::hisG-URA3-hisG*, *his4*, *leu2*, *trp1*, *ura3*) or ORD7254-25D (*MAT* α , *his4*, *leu2*, *trp1*, *ura3*) and verified by Southern blot analysis. gRNA expression plasmids were introduced into yeast cells by electroporation and transformants were selected on plates depleted in leucine. The *sae2* Δ , *spo11* Δ and *gal4* Δ mutations were introduced by genetic crossing using appropriate and previously described haploid strains (21).

Site-directed mutagenesis of the *QQR* RS located in the *RSC9-MSCI* intergenic region was carried out using the Quick Change Site-directed Mutagenesis Kit (Stratagene) by mutating the GGG GAA GAA RS sequence into GGG GAT TAA, thus creating an *AseI* site. This mutation (*iRSC9-MSCI* RS-*AseI*) was integrated into the yeast genome by two-step transformation and verified by Southern blot analysis.

The *NatMX* and *HphMX* resistant cassettes were PCR-amplified from plasmids pAG25 (36) and pMJ696 (identical to pAG32 (36)) and flanked by the yeast targeting regions of homology. To measure recombination frequencies around the *GAL2* locus, the *NatMX* and *HphMX* cassettes were integrated in the terminator of *GAL2* (*GAL2ter*) between positions 292068 and 292069 and in the promoter of *EMP46* (*EMP46prom*) between positions 287725 and 287726 on chromosome XII, respectively. To examine the frequency of meiotic recombination near the *PUT4* locus, *NatMX* and *HphMX* cassettes were inserted into the intergenic i(*REV1-*

PYK2) and i(*PUT4-CIN1*) regions of chromosome XV at position 984842–984843 and 989657–989658, respectively. To study the effects of *TECI-SPO11* expression on meiotic recombination, the *NatMX* and *HphMX* cassettes were integrated in the promoter of the *COX5A* and *VAC7* genes on chromosome XIV at positions 525932–525933 and 531522–531523, respectively. To examine the frequency of meiotic recombination around the *HHT2-HHF2* region in chromosome XIV, the *NatMX* and *HphMX* cassettes were inserted between positions 574156 and 574157, and 578751 and 578752, respectively. To determine recombination frequencies around the *MSC1* locus, the *KanMX* and *HphMX* markers were inserted into the intergenic i(*PGA3-ERG13*) and i(*COX14-ERO1*) regions at position 20682–20692 and 14249–14300 on chromosome XIII, respectively. The expected chromosomal integration sites were verified by junction PCR and Southern blotting.

Sporulation conditions

For meiotic time-courses, diploid cells were grown at 30°C in SPS presporulation medium and transferred into the sporulation medium (1% potassium acetate supplemented with amino acids) as previously described (37). Sporulation was performed at 30°C, 250 rpm. Tetrads were dissected after 96 h of sporulation.

Chromatin immunoprecipitation

ChIP experiments were performed as previously described (26). Briefly, about 8×10^8 meiotic *CRISPR-dCAS9-SPO11 spo11* Δ /*spo11* Δ *sae2* Δ /*sae2* Δ cells were treated with 1% formaldehyde for 15 min at room temperature and then 125 mM Glycin for 5 min. Immunoprecipitation was performed using 2 μ g of the ANTI-FLAG mouse antibodies (Clone M2; Sigma-Aldrich) in combination with 35 μ l of magnetic Dynabeads protein G (panMouse IgG, Dynal). Quantitation of immunoprecipitated DNA was performed via real-time quantitative PCR analysis, using Power SYBR Green mix (Applied Biosystems) and a 7900HT Fast Real-Time PCR System (Applied Biosystems). Quantitative PCR was performed on 1/60 of the immunoprecipitate or 1/20 000 of the whole-cell extract, and analyzed as described (37). To determine the non-specific background the amount of the *SMCI* DSB-cold domain (38) was measured in each immunoprecipitate. Fold enrichments are expressed as the relative fold enrichment of target site over *SMCI* signal and are normalized to input DNA. Sequence of the qPCR primers are listed in the Supplementary Table S1.

DSB mapping and quantification

Physical DSB detection was performed in strains homozygous for the *sae2* allele (or the *rad50S* allele for *QQR* strains) to allow the accumulation of unrepaired DSBs. Genomic DNA was extracted as previously described (25). For Southern blot detection of 1 to 15 kb DNA fragments, genomic DNA or agarose-embedded DNA from meiotic samples was digested with appropriate restriction enzymes and the resulting fragments were separated by electrophoresis in 0.8–1.5% agarose gels and transferred under vacuum

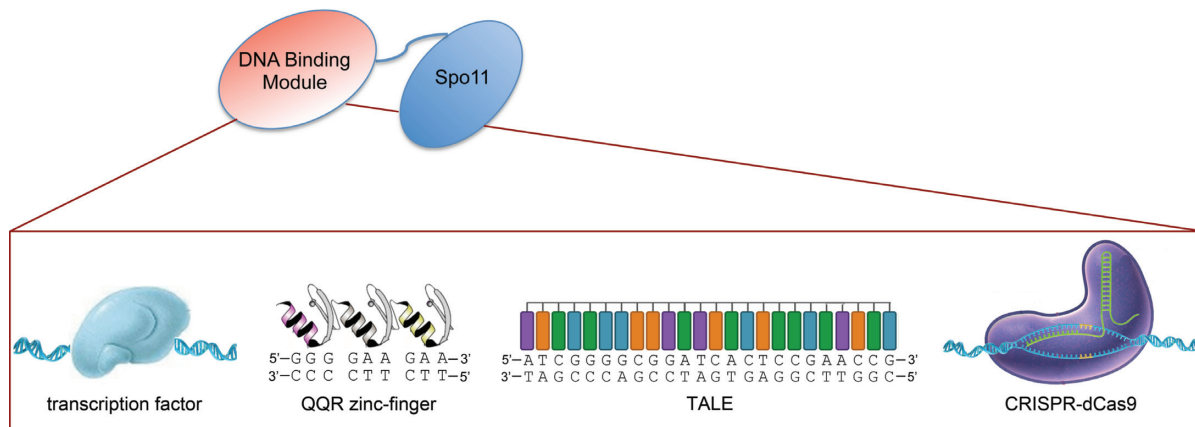


Figure 1. Architecture of the targeting Spo11 fusions. To target meiotic DSB formation, the DSB-promoting Spo11 transesterase was fused to various DNA binding modules. Four different non-programmable Spo11 fusions were designed upon conjugation with the Gal4, Tec1 or Rsc3 transcription factors, or to the centromere-associated Mtw1 protein. Three programmable Spo11 fusions were constructed with an artificial zinc-finger array, a TALE polypeptide, or the CRISPR dCas9 protein. Other functional features of these DNA-binding modules are indicated in Supplementary Table S3.

(Appligene) onto Hybond XL membranes (Amersham). DNA probes were PCR-amplified from genomic DNA and were labelled by ^{32}P -dCTP using the Ready Prime kit (GE Healthcare). Probe hybridization of the membrane was performed as described previously (39). Parental and DSB bands were visualized by using a Typhoon 9400 Phosphoimager (GE Healthcare) and quantified with the ImageJ (NIH) software. DSB frequencies were measured as % of radioactivity in each DSB fragment relative to the total amount of radioactivity in the parental plus DSBs bands. For the majority of examined regions two independent experiments were performed to determine DSB frequencies. In these cases DSB values are the average of two experiments.

Yeast strains, restriction enzymes and probes are as follows:

Figure 2: genomic DNA was prepared from *SPO11/SPO11* (ORD7304), *GAL4-SPO11/GAL4-SPO11 spo11Δ/spo11Δ* (AND2096), *TEC1-SPO11/TEC1-SPO11 spo11Δ/spo11Δ* (AND1926), *RSC3-SPO11/RSC3-SPO11 spo11Δ/spo11Δ* (AND2006), *TALE-SPO11/TALE-SPO11 spo11Δ/spo11Δ* (AND2529), *QQR-SPO11/QQR-SPO11 spo11Δ/spo11Δ* (ORD8146), *SPO11/SPO11 + gRNA-YCR048W-Gal4_{UAS1}* (ANT2524), *dCAS9-SPO11/0 + gRNA-handle spo11Δ/spo11Δ* (ANT2527) and *dCAS9-SPO11/0 + gRNA-YCR048W-Gal4_{UAS1} spo11Δ/spo11Δ* (ANT2528) diploids, digested with *AseI* and probed with an internal *YCR048W* fragment.

Figure 3A: genomic DNA was prepared from *SPO11/SPO11 GAL4/GAL4* (ORD7304), *SPO11/SPO11 gal4Δ/gal4Δ* (AND2599), *GAL4-SPO11/GAL4-SPO11 spo11Δ/spo11Δ GAL4/GAL4* (AND2096), *GAL4-SPO11/GAL4-SPO11 spo11Δ/spo11Δ gal4Δ/gal4Δ* (AND1969), *TALE-SPO11/TALE-SPO11 spo11Δ/spo11Δ GAL4/GAL4* (AND2529) and *TALE-SPO11/TALE-SPO11 spo11Δ/spo11Δ gal4Δ/gal4Δ* (AND2540) diploids, digested with *XbaI* and probed with a *GAL2* fragment.

Figure 3B: genomic DNA was prepared from *dCAS9-SPO11/0 + gRNA-handle spo11Δ/spo11Δ* (ANT2527), *dCAS9-SPO11/0 + gRNA-handle spo11Δ/spo11Δ gal4Δ/gal4Δ* (ANT2536), *dCAS9-SPO11/0 + gRNA-GAL2prom-Gal4_{UAS-A} spo11Δ/spo11Δ* (ANT2532), *dCAS9-SPO11/0 + gRNA-GAL2prom-Gal4_{UAS-A} spo11Δ/spo11Δ gal4Δ/gal4Δ* (ANT2534), *dCAS9-SPO11/0 + gRNA-GAL2prom-Gal4_{UAS-B} spo11Δ/spo11Δ* (ANT2531), *dCAS9-SPO11/0 + gRNA-GAL2prom-Gal4_{UAS-B} spo11Δ/spo11Δ gal4Δ/gal4Δ* (ANT2535), *dCAS9-SPO11/0 + gRNA-GAL2prom-Gal4_{UAS-D/E} spo11Δ/spo11Δ* (ANT2530), *dCAS9-SPO11/0 + gRNA-GAL2prom-Gal4_{UAS-D/E} spo11Δ/spo11Δ gal4Δ/gal4Δ* (ANT2533), *dCAS9-SPO11/0 + gRNAs targeting GAL2prom-Gal4_{UAS-A,-B,-D/E} spo11Δ/spo11Δ* (ANT2551) and *gRNAs targeting GAL2prom-Gal4_{UAS-A,-B,-D/E} spo11Δ/spo11Δ gal4Δ/gal4Δ* (ANT2552) diploids, digested with *XbaI* and probed with an internal *GAL2* fragment.

Figure 4A: genomic DNA was prepared from *SPO11/SPO11* (ORD7304) and *TEC1-SPO11/TEC1-SPO11 spo11Δ/spo11Δ* (AND1926) diploids, digested with *PstI* and probed with an internal *MSG5* fragment.

Figure 4B: genomic DNA was prepared from *SPO11/SPO11* (ORD7304) and *RSC3-SPO11/RSC3-SPO11 spo11Δ/spo11Δ* (AND2006) diploids, digested with *PstI* and probed with a *SIW14* fragment.

Figure 4C: genomic DNA was prepared from *SPO11/SPO11* (ORD7239), *QQR-SPO11/QQR-SPO11 spo11Δ/spo11Δ* (RS/RS) (ORD8146), *QQR-SPO11/QQR-SPO11 spo11Δ/spo11Δ* (RS/rs) (ORD8683) and *QQR-SPO11/QQR-SPO11 spo11Δ/spo11Δ* (rs/rs) (ORD8694) diploids, digested with *HincII* and probed with an *RSC9* fragment.

Figure 4D: genomic DNA was prepared from *SPO11/SPO11* (ORD7304), *dCAS9-SPO11/0 + gRNA-handle spo11Δ/spo11Δ* (ANT2527) and *dCAS9-SPO11/0 + gRNA-MSCIprom spo11Δ/spo11Δ* (ANT2708) diploids, digested with *AseI* and probed with a *MSCI* fragment.

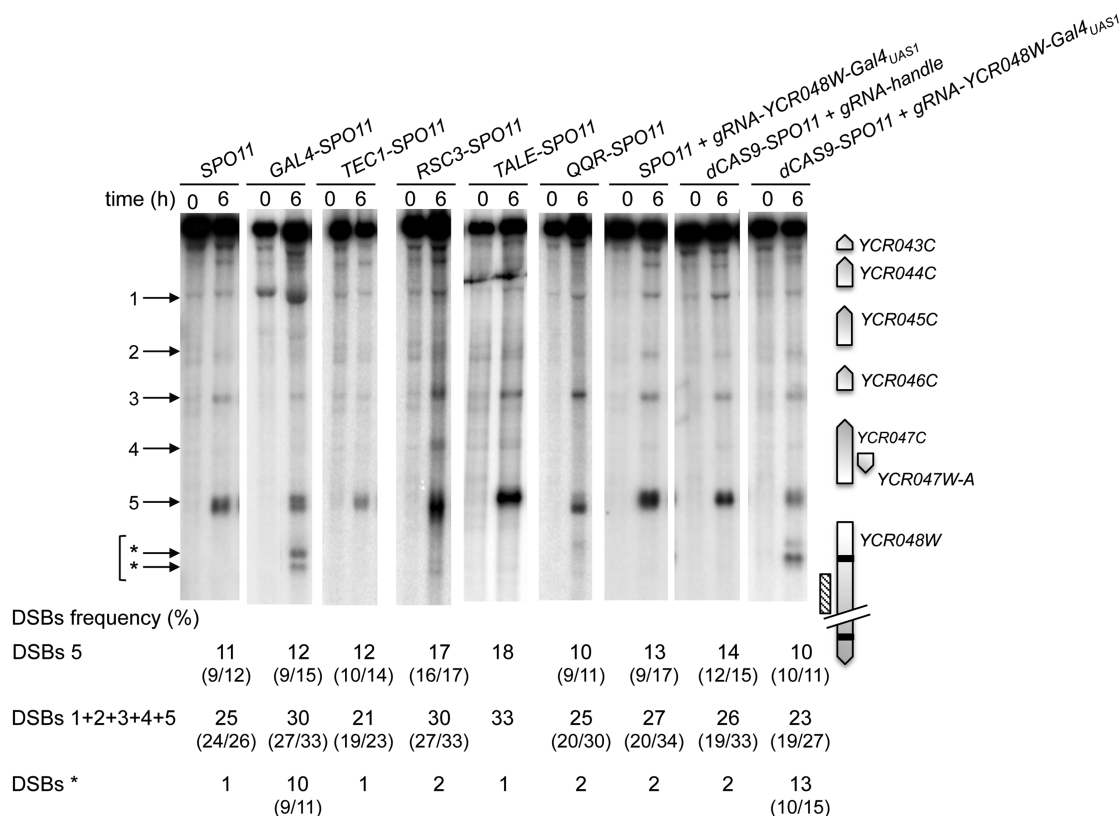


Figure 2. Targeting Spo11 fusions trigger DSB formation in the natural hotspot *YCR043C-YCR048W* region. DSB formation was analyzed by Southern blot in cells harvested 0 and 6 h after transfer into sporulation medium. At the right of the blot, a map shows the ORFs (open arrows indicate transcriptional sense) and the position of the probe (hatched rectangle). Target Gal_{UAS1} and Gal_{UAS2} sites are shown as black bars. At the left of the blot, arrowheads indicate wild-type (numbered) and Gal4-Spo11 and dCas9-Spo11 targeted DSBs (asterisks). DSB frequencies (percentage of DSB fragment per total DNA) listed under each lane correspond to the mean of two independent experiments with minimum and maximum values indicated into parentheses, excepted for TALE-SPO11 (a single experiment was performed). The sum of DSB frequencies in the *YCR044C* (1), *YCR045C* (2), *YCR046C* (3), *YCR047W-A* (4), and *YCR047C-YCR048W* (5) promoters account for $\geq 95\%$ of the total DSBs detected in the *YCR043C-YCR048W* region. Frequency of DSBs* corresponds to the sum of frequencies detected in the *YCR048W* ORF (indicated by *arrows).

Figure 6A: genomic DNA was prepared from *SPO11/SPO11* (ORD7304), *dCAS9-SPO11/0 spo11Δ/spo11Δ* + gRNA-handle (ANT2527), *GAL4-SPO11/GAL4-SPO11 spo11Δ/spo11Δ* (AND2096), *dCAS9-SPO11/0 spo11Δ/spo11Δ* + gRNA-*YCR048W*-Gal4_{UAS1} (ANT2559) and *dCAS9-SPO11/0 spo11Δ/spo11Δ* + gRNA-*YCR048W*-Gal4_{UAS2} (ANT2528) diploids, digested with *AseI* and *SacI* and probed with a *YCR048W-YCR051W* fragment.

Figure 6B: genomic DNA was prepared from *SPO11/SPO11* (ORD7304), *dCAS9-SPO11/0 spo11Δ/spo11Δ* + gRNA-handle (ANT2527) and *dCAS9-SPO11/0 spo11Δ/spo11Δ* + gRNA-*SWC3* (ANT2564) diploids, digested with *AvrII* and *PacI* and probed with a *MDM10-SPO7* fragment.

Figure 6C: genomic DNA was prepared from *SPO11/SPO11 GAL4/GAL4* (ORD7304), *dCAS9-SPO11/0* + gRNA-handle *spo11Δ/spo11Δ GAL4/GAL4* (ANT2527), *dCAS9-SPO11/0* + gRNA-*PUT4*-Gal4_{UAS} *spo11Δ/spo11Δ GAL4/GAL4* (ANT2547), *dCAS9-SPO11/0* + gRNA-*PUT4*-Gal4_{UAS} *spo11Δ/spo11Δ gal4Δ/gal4Δ* (ANT2553), *GAL4-SPO11/GAL4-SPO11 spo11Δ/spo11Δ GAL4/GAL4* (AND2096) and *GAL4-*

SPO11/GAL4-SPO11 spo11Δ/spo11Δ gal4Δ/gal4Δ (AND1969) diploids, digested with *BamHI* and *XhoI* and probed with a *CINI* fragment.

RESULTS

Design of targeting Spo11 fusions

To direct Spo11 to various sites in the *Saccharomyces cerevisiae* genome, we fused the N-terminal region of the full length ScSPO11 gene to various DNA-binding modules and expressed the constructs under the *ADH1* constitutive promoter (Figure 1 and Materials and Methods). To use the CRISPR system, we similarly integrated the *P_{ADH1}-dCAS9-SPO11* construct at the *TRP1* locus and expressed gRNA(s) on a high-copy 2 μ plasmid (Materials and Methods). As a negative control, we used a gRNA lacking the 20-nt guide sequence (gRNA handle) but able to form the ribonucleoprotein complex (40). Unless specified, the performance of the fusion constructs was examined in diploid cells deleted for the endogenous *SPO11* gene. Altogether, we generated four ‘non-programmable’ Spo11 fusions with the full-length transcription factor proteins Gal4, Tec1 and Rsc3, that recognize distinct genomic targets, or Mtw1, a subunit of the

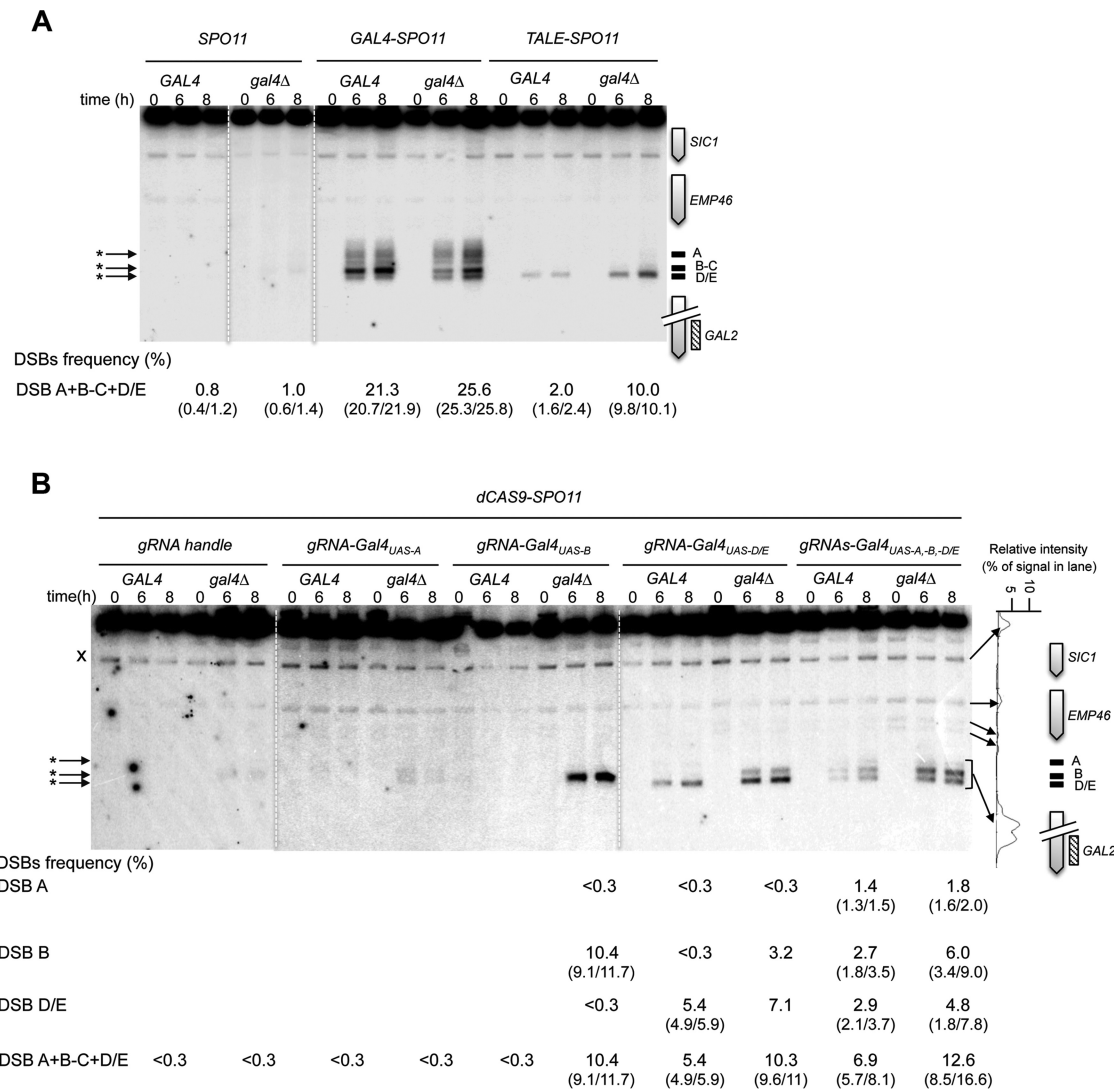


Figure 3. Gal4-, TALE- and dCas9-Spo11 fusions promote DSBs in the targeted DSB-cold *GAL2* promoter. Southern blot analysis of DSBs targeted by Gal4- and TALE-Spo11 (A), and dCas9-Spo11 (B) at the *GAL2* promoter in *GAL4* and *gal4Δ* cells. TSF target sites are shown as black bars at the right of the gel and arrowheads indicate TSF-induced DSBs (asterisks) at the left of the gel; crosses indicate cross hybridizing bands. The profile of DSB quantification in *dCAS9-SPO11 gal4Δ* diploids expressing multiple gRNAs directed against the *GAL2* promoter ($t = 8$ h) is shown to the right of the panel B. DSB values are from single experiments or the mean of two independent experiments with minimum and maximum values indicated into parentheses.

kinetochore MIND protein complex (Supplementary Table S3). In addition, we built three ‘programmable’ TSFs using an artificial three zinc-finger DNA-binding array (QQR) (41), a TALE DNA-binding array (42,43) or the *Streptococcus pyogenes* nuclease-dead Cas9 D10A/H840A protein (dCas9) (32). QQR has 149 potential GGGGAAGAA binding sites in the yeast genome. The TALE was designed to bind a unique 25-nt target sequence (Gal4_{UAS-D/E}) located within the promoter of the *GAL2* gene. The 20-bp targets of dCas9-Spo11 were specified with various gRNAs (Supplementary Table S2).

The Spo11 fusions are functional

In the *S. cerevisiae* SK1 strain background, spore viability is very high (>90%) and is abolished in the *spo11Δ* mutant (Table 1). All of the *SPO11* fusion constructs, expressed in

one or two copies, restored >90% spore viability (Table 1). This demonstrates that the Spo11 moiety of the fusions is functional and allows the formation of a sufficient number of crossovers per chromosome to ensure their proper segregation during meiosis.

DSB formation at natural sites

Next, we investigated whether the Spo11 fusions retain the ability to promote meiotic DSB formation in a natural DSB region. We examined the well characterized *YCR043C-YCR048W* region of chromosome III (44,45) that exhibits DSBs in several promoters. All TSF strains display meiotic DSBs at the same locations as in the wild-type (*SPO11*) strain within this 9-kb region, with the total DSB frequency varying between 21 and 33% (Figure 2). The *YCR048W* DSB hotspot (DSB#5) remains the strongest in all strains,

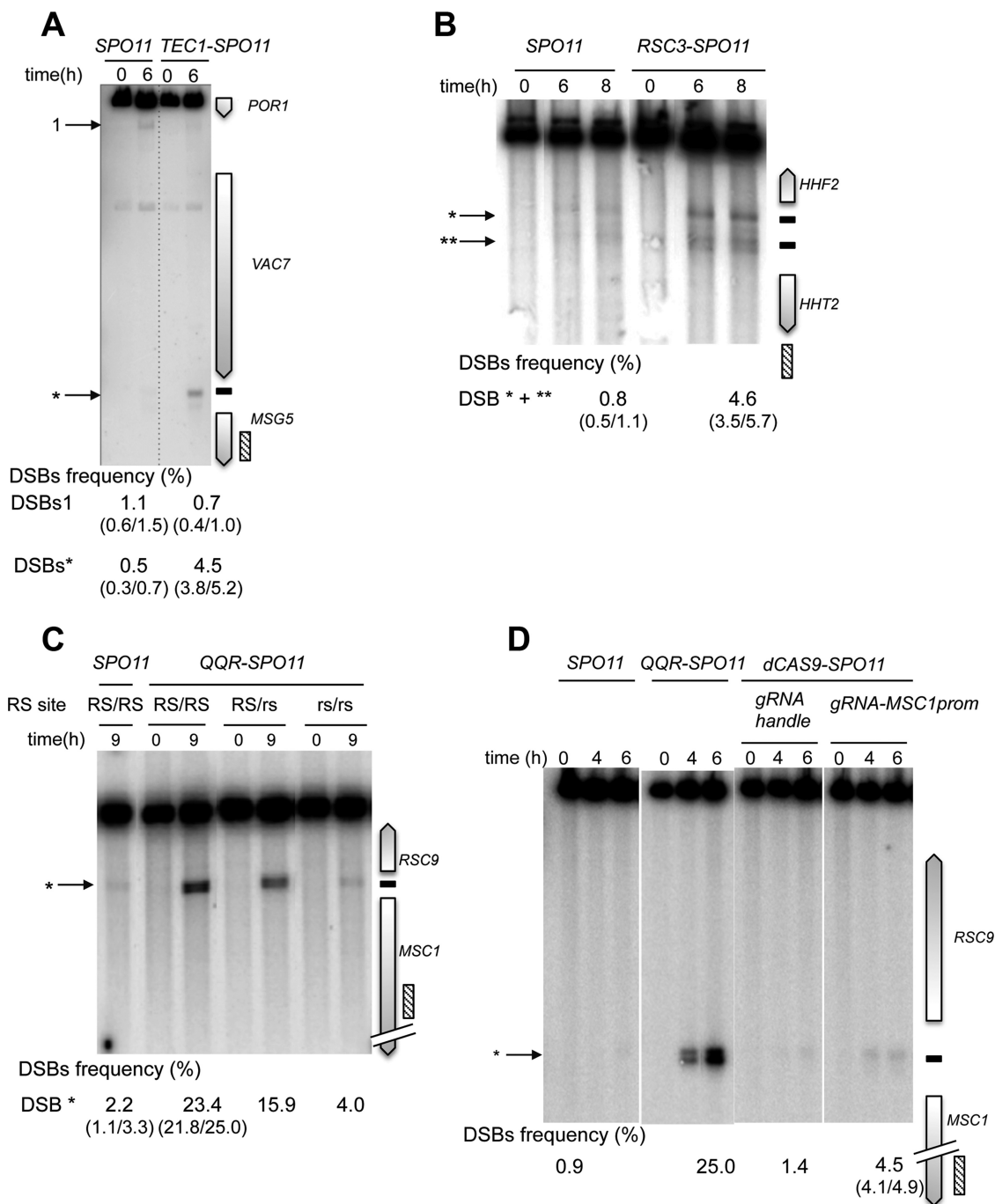


Figure 4. Tec1-, Rsc3 and QQR-Spo11 fusions stimulate DSB formation in targeted DSB-cold promoter-containing regions. Southern blot analysis of DSBs targeted by Tec1-Spo11 at the *MSG5* promoter (A), Rsc3-Spo11 at the *HHF2-HHT2* promoter region (B) and QQR-Spo11 and dCas9-Spo11 at the *RSC9-MSI1* promoters (C and D). TSF target sites are shown as black bars at the right of the gel and arrowheads indicate wild-type (numbered) and TSF-induced DSBs (asterisks) at the left of the gel. The presence of the homozygous wild-type QQR recognition site (RS), heterozygous mutated RS (RS/rs) and homozygous mutated RS (rs/rs) is indicated in panel C. DSB values as described in Figure 3 legends.

ranging between 10–18% (11% in the *SPO11* strain). The Gal4-Spo11 and dCas9-Spo11 (with gRNA_{UAS1}) fusions also induce DSBs at a new site within the *YCR048W* coding sequence, where they have a specific binding sequence (see below).

DSB formation in cold promoter regions

In yeasts, 90% of DSB hotspots cluster in intergenic regions containing promoters, and only ~15% of the promoters exhibit strong hotspots (5,18). To investigate the capacity of the Spo11 fusions to mediate DSB formation in promoters that naturally exhibit low or undetectable DSBs, we examined several promoter-containing regions for each con-

Table 1. Targetable Spo11 fusions yield viable meiotic products

TSF gene construct	Spore viability (%)	
	One copy	Two copies
<i>SPO11</i>	—	98 (53)
<i>spo11</i>	93 (22)	0 (32)
<i>GAL4BD-SPO11</i>	ND	96 (138) ^a
<i>GAL4-SPO11</i>	94 (18)	92 (22)
<i>TEC1-SPO11</i>	88 (22)	92 (22)
<i>RSC3-SPO11</i>	93 (21)	93 (21)
<i>MTW1-SPO11</i>	100 (22)	98 (24)
<i>TALE-SPO11</i>	97 (35)	95 (15)
<i>QQR-SPO11</i>	97 (24)	96 (24)
<i>dCAS9-SPO11</i>	93 (60)	92 (22)

Tetrads from diploid strains were dissected and spore viability was measured (%). The number of tetrads dissected is reported in parentheses. All strains harbouring one or 2 copies of the Spo11 fusion gene construct were built in a *spo11Δ/spo11Δ* genetic background.

^adata from (21). ND: not determined.

struct. Remarkably, the Gal4-, Tec1- and Rsc3-Spo11 fusions stimulated the frequency of DSB formation 10–26, 9–14 and 6–12 fold, respectively, in the targeted regions (Figures 3 and 4 and Supplementary Figure S2). Like Gal4BD-Spo11 (25,26), Gal4-Spo11 induces multiple DSBs in the promoter of the *GAL2* gene that contains five partially overlapping Gal4_{UAS} sites (Figure 3A). In the absence of the native Gal4 protein, we found that the DSB frequency was slightly enhanced from 21.3 to 25.6% (see below for detailed description of the target-binding competition of the endogenous Gal4 protein). Rsc3-Spo11 and Tec1-Spo11 precisely target two adjacent sites present in the *HHF2-HHT2* and *TEC1-UBC4* promoters, respectively (Figure 4B and Supplementary Figure S2).

Regarding the programmable Spo11 fusions, QQR-Spo11 also strongly stimulates DSB formation in regions that contain a recognition site. Namely, it increases 10-fold (2.2–23.4%) within the *RSC9-MSC1* promoter region (Figure 4C) and 4-fold (2.0 versus 8.0%) in the *ESII-HOF1* promoter region, where it overlaps a natural DSB site (Supplementary Figure S3A). In the *SUTI-RAD54* promoter region QQR-Spo11 triggers additional DSBs in the vicinity of the target site (Supplementary Figure S3B); the DSB#1 is located near a 1 bp variant QQR site (GGGGAAGAC). The other DSBs are weaker and unexpected. It can result from a local positive *cis*-effect increasing chromatin accessibility near the target site or from the local interaction of QQR with unidentified chromatin/DNA associated proteins. To test QQR target specificity, we mutated two triplets of the QQR recognition site (RS) located in the *RSC9-MSC1* region. In the strain heterozygous for the target site (RS/rs), DSB formation was reduced from 23.4 to 15.9% and was further reduced near the wild type level (4.0%) in the rs/rs strain mutated on both homologs (Figure 4C), demonstrating that QQR-Spo11 recognizes the expected target sequence *in vivo*. Concerning targeting Spo11 with a TALE module, DSB frequency only slightly increases (0.8 versus 2.0%) at the Gal4_{UAS-D/E} target site located within the *GAL2* promoter (Figure 3A), due to endogenous binding competition (see below). DSB formation was abolished upon mutation of its binding sequence (Supplementary Fig-

ure S4A). Based on these results, we concluded that the QQR and TALE programmable modules also allow the functional targeting of Spo11.

Then, to test dCas9-Spo11 and compare its efficiency to QQR-, Gal4- and TALE-Spo11 DSB formation in the same region, we designed several gRNAs matching the QQR and Gal4 binding sites in the *RSC9-MSC1* and *GAL2* promoter regions, respectively. Directing dCas9-Spo11 to the QQR binding site led to a 3-fold increase of DSB frequency at the target site (1.4 versus 4.5%; Figure 4D). In the *GAL2* promoter, co-expression of dCas9-Spo11 with a gRNA-Gal4_{UAS-D/E} led to a 18-fold stimulation of targeted DSBs (5.4%) compared to the controls (<0.3%), but surprisingly, targeting of the adjacent Gal4_{UAS-A} and Gal4_{UAS-B} sites was not efficient (Figure 3B). However, multiplex targeting of the Gal4_{UAS-A, -B, -D/E} sites resulted in an enhanced DSB frequency (6.9%) distributed in three discrete bands, whose migration corresponds to DSB formation at each target site (Figure 3B). For comparison, the total DSB frequency in the *GAL2* promoter appears the highest in the *GAL4-SPO11* strain (21.3%) with five target Gal4_{UAS} binding sites, intermediate in the *dCAS9-SPO11* strain (up to 6.9% upon multiplex targeting) and weak in the *TALE-SPO11* strain (2.0%) targeting the single Gal4_{UAS-D/E} site.

Altogether these results demonstrate that distinct DNA binding modules, i.e. full length transcription factors, synthetic Zn fingers, TALE domains and dCas9, can be conjugated to Spo11 in order to induce meiotic DSB formation in various DSB-cold promoters harbouring a binding site, but local- and module-specific variations in efficiency are observed.

Competition with endogenous factors modulates the targeting efficiency

One potential limitation to targeting DSBs with Spo11 fusions is the local competition with endogenous DNA- or chromatin-binding protein(s). *In vitro* studies have shown that the Gal4 protein displays nanomolar affinity for the consensus Gal4_{UAS} binding sequences (46,47). To investigate whether the native Gal4 protein interferes with targeting the Gal4_{UAS}, we expressed the Gal4-, TALE- and dCas9-Spo11 fusions in strains deleted for the endogenous *GAL4* gene. As a control, deletion of *GAL4* in the *SPO11* strain had no stimulating effect (Figure 3A). In contrast, the Gal4-Spo11 DSB frequency was slightly enhanced at the targeted *GAL2* promoter (from 21.3 to 25.6%) as previously observed for Gal4BD-Spo11 (48). Similarly, DSBs generated by Gal4-Spo11 at the *GAL7* and *GAL1-GAL10* promoters was increased 2.8- and 4.4-fold, respectively, in the *gal4Δ* strain (Supplementary Figure S2A). The targeting of DSBs at the *GAL2* Gal4_{UAS-D/E} site by TALE-Spo11 was enhanced 5-fold (up to 10%) in the absence of the native Gal4 protein (Figure 3A and Supplementary Figure S4A). As expected, TALE-Spo11 DSBs were barely (1.5%) or not detectable in the *GAL2-abcdE* strain mutated for the TALE binding sequence and at the other Gal4_{UAS} sites located in the *GAL1/GAL10* and *GAL7* promoters (Supplementary Figure S4A and B). As a positive control, Gal4-Spo11 strongly targets DSBs in the *GAL2-abcdE* strain which retains only the Gal4_{UAS-E} binding site. These results demon-

strate the target specificity of the TALE array in recognizing a unique 24-bp sequence. Similarly, DSBs induced by dCas9-Spo11, using single or multiple gRNAs targeting the *GAL2* Gal4_{UAS} sites, were enhanced up to 40-fold (<0.3% versus 12.6%) in the *gal4Δ* mutant (Figure 3B). These results suggest that the native Gal4 protein acts as a strong competitor for the binding of the relevant Gal4-, TALE- and dCas9-Spo11 fusions.

Finally, to assess whether the endogenous competition by Gal4 results from reduced binding of the Spo11 fusion proteins to the target sites, we performed ChIP-qPCR assays of the dCas9-Spo11-3xFLAG construct using an anti-FLAG antibody (Materials and Methods). In the most efficient DSB-targeting situation, i.e. dCas9-Spo11 expressed with multiple gRNAs, we readily detected chromatin binding of dCas9-Spo11 at the *GAL2* locus at the onset of meiosis ($t = 0$ h) and observed the expected increase in association during the prophase of meiosis, reaching a 3-fold higher level at $t = 6$ h, when DSB formation occurs (Figure 5A). The gRNA handle control showed no dCas9-Spo11 binding. The binding of dCas9-Spo11 upon co-expression of the gRNA-Gal4_{UAS-A} and gRNA-Gal4_{UAS-B} was low and increased 2- and 7-fold upon removal of the Gal4 protein (Figure 5B), respectively. Mechanistically, these results indicate that the binding of CRISPR-dCas9-Spo11 to the target site is not sufficient for cleavage (Gal4_{UAS-A}) and is sensitive to the competition with an endogenous protein (Gal4_{UAS-B}).

DSB induction in coding regions

In yeasts, <5% of the DSB hotspots are located in non-promoter regions (5,18). To assay the performance of the various targeting strategies, we first examined DSB formation in the *YCR048W* coding region that contains two Gal4 consensus binding sequences, Gal4_{UAS1} and Gal4_{UAS2}, located at the beginning and the end of the coding region, respectively. In *SPO11* diploids, rare DSBs (1%) are detected near the *YCR048W*-Gal4_{UAS1} (Figure 2). However, like Gal4BD-Spo11 (21), Gal4-Spo11 and dCas9-Spo11 stimulate DSB formation at the Gal4_{UAS1} site (up to 13-fold) (Figure 2). As controls, co-expression of dCas9-Spo11 and a gRNA handle in *spo11Δ* cells, as well as the sole expression of the gRNA-*YCR048W*-Gal4_{UAS1} in *SPO11* cells failed to stimulate DSB formation in this coding region. Concerning the downstream Gal4_{UAS2}, neither Gal4BD-Spo11 nor Gal4-Spo11 stimulates DSBs at this site [(21) and Figure 6A]. However, cleavage is slightly enhanced in cells co-expressing dCas9-Spo11 and the gRNA-*YCR048W*-Gal4_{UAS2}, reaching 2.3%.

Next, we examined the targeting efficiency of dCas9-Spo11-mediated DSBs in the cold *SWC3* coding region located a gene away from the natural *CYS3* and *DEP1-SYN8* hot spots (49). Remarkably, the strain expressing the dCas9-Spo11 and gRNA-*SWC3* strongly induces DSB formation in the targeted region (0.6% versus 4.2%), while retaining DSBs in the *CYS3* and *DEP1* promoters as in wild type (Figure 6B). We also designed gRNAs directed against the Gal4_{UAS} sites contained in the *GAL2*, *PUT4*, *NCE102* and *YPR1* genes located in naturally cold regions (26). DSB formation in the *PUT4* region is weak in the wild-type strain (1.6%) but is strongly stimulated by Gal4-Spo11

in the presence or absence of the Gal4 protein, reaching 12.9 and 15.9%, respectively (Figure 6C). In contrast, removal of Gal4 was required to stimulate DSB formation by dCas9-Spo11, reaching 4.4%. This dependency is consistent with the high level of dCas9-Spo11 chromatin binding to the *PUT4*-Gal4_{UAS} target (8-fold enrichment over background), only in the absence of Gal4 (Figure 5B). No Gal4-Spo11 nor dCas9-Spo11 targeted DSBs were observed in the coding region of the *GAL2*, *NCE102* and *YPR1* genes, in the presence or absence of Gal4 (Supplementary Figure S5). Altogether, these results demonstrate that DSB formation can be stimulated in coding regions, but the performance is heterogeneous.

Targeting of DSB refractory regions

Next, we examined the targeting of dCas9-Spo11 in other known DSB-rare regions. No targeted DSB formation was observed in the terminator regions of the *SWC3* and *GAL2* genes (Supplementary Figure S6), albeit dCas9-Spo11 associates with the latter locus (Figure 5B). We also attempted to stimulate DSB formation in pericentric regions that are universally cold for DSB formation (5,7,14,18,26,50,51). Neither natural nor targeted DSBs were observed in the *SNF8* gene located 1.8 kb from *CEN16* (Supplementary Figure S7A), in agreement with the lack of chromatin binding (Figure 5B). Whereas dCas9-Spo11 binds to the Gal4_{UAS}-containing *GAL3* region (located 13 kb from the centromere of chromosome IV) in a Gal4p-independent manner (Figure 5B), no natural nor targeted DSB formation was detected (Supplementary Figure S7D). We also built a fusion of Spo11 to the centromere-associated Mtw1 protein, a non-essential component of the kinetochore complex (52) (Supplementary Table S3). Albeit expression of Mtw1-Spo11 restored spore viability in the absence of Spo11 (Table 1), no DSB formation was detected near the centromere of chromosomes XVI and III (Supplementary Figure S7B and C). These results confirm the strong inhibitory effects on DSB formation exerted by a centromere (26,50,53,54).

Subtelomere regions are cold in yeast but rather recombination proficient in other eukaryotes, including plants and mammals (17,55). We designed a gRNA to direct dCas9-Spo11 to a unique subtelomeric sequence located ~10 kb from the end of chromosome II. Neither chromatin binding nor DSB formation was detected in the targeted *MAL31* promoter region (Figure 5B and Supplementary Figure S8). Finally, to attempt the targeting of a repeated sequence of the yeast genome, we assayed the targeting of Spo11 to the ~330-bp long terminal repeat (LTR) sequences which flank the transposable Ty elements (30 copies per SK1 cell (56)). The Tys are located in various naturally DSB-prone or -cold regions of the genome, nevertheless with the common feature that they are internally cold but not fully refractory (56). We programmed a single gRNA to match a unique 20-nt sequence conserved in the LTR sequence of 11 Tys (56) and examined DSB formation in two different genomic contexts. In the *TYPEX25-CARI* region natural DSB formation was slightly enhanced near the 5' LTR (15.8 versus 25.3%) but no DSBs were detected in both targeted 5' and 3' LTRs *per se* (Supplementary Figure S9A-B). In contrast, in the naturally cold *TyCUS2-MRP10* region, we observed a 3-fold

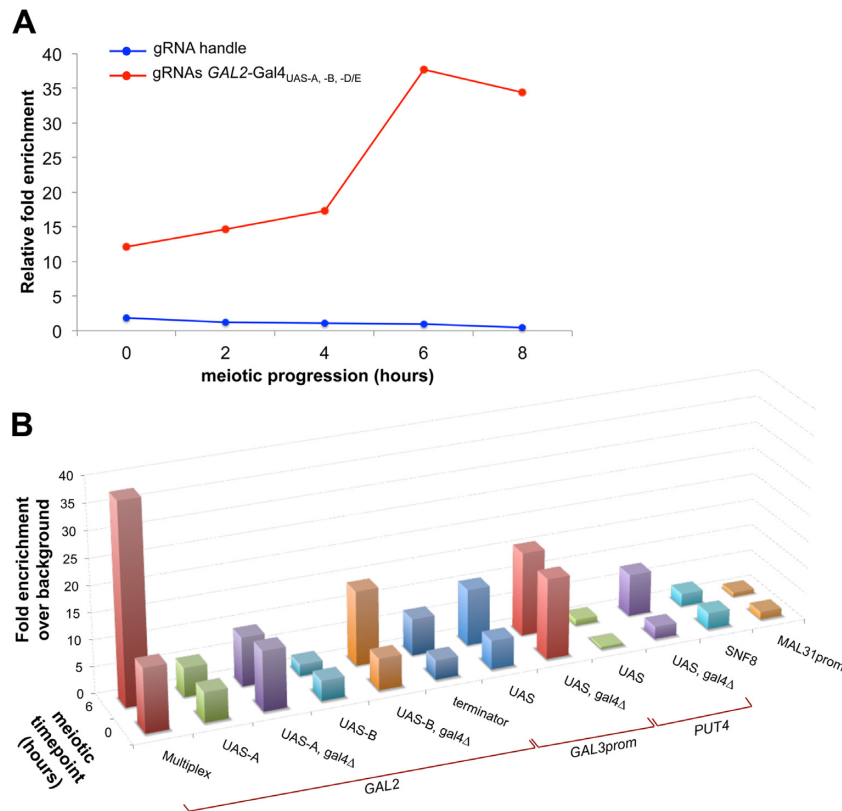


Figure 5. dCas9-Spo11 fusion binding at various genomic loci. Quantitative analysis of dCas9-Spo11 association with the target *GAL2* promoter upon expression of the gRNA handle or multiple gRNAs (A), and with various genomic loci upon expression of the corresponding gRNAs (B), was assessed by Chromatin immunoprecipitation (ChIP) in *sae2 Δ* diploids expressing the Flag-tagged dCas9-Spo11 protein. Cells were collected at the indicated times after transfer to sporulation medium ($t = 0$ h), fixed with formaldehyde *in vivo* and immunoprecipitated with anti-flag antibodies. Quantitation of immunoprecipitated DNA was performed via qPCR and fold enrichments are expressed as the relative fold enrichment of target site over *SMC1* signal and are normalized to input DNA (Materials and Methods). In the panel B the enrichment for each target site was normalized to the fold enrichment measured in control *gRNA handle-dCAS9-SPO11* cells.

increase (0.4 versus 1.3%) in DSB formation within the 5' LTR (Supplementary Figure S9C). No DSB formation was detected in the 3' LTR (Supplementary Figure S9D).

These results show that the targeting of DSBs remains inefficient in certain regions of the genome even with dCas9-Spo11, indicating that unlocking DSB formation in these refractory regions will require other strategies.

DSB targeting locally enhances crossover frequency

To verify that the targeted stimulation of DSB formation enhances meiotic recombination frequencies, we introduced flanking heterozygous markers in several chromosomal regions and measured the meiotic recombination rates in the progenies of each TSF strain, upon dissection of four-spore tetrads. In all cases, except negative controls, we observed a significant 2- to 6-fold stimulation of crossovers (calculated as cM/kb). This was true for the Spo11 fusions with Gal4, Tec1, Rsc3, QQR, TALE and dCas9 (Table 2) at sites where DSB formation was observed. For comparison, in the *GAL2* region, Gal4BD- and Gal4-Spo11 fusions resulted in a 5.4- and 5.0-fold stimulation of crossovers compared to the wild type *SPO11* strain while TALE-Spo11 (in the most stimulating *gal4 Δ* context) and the single and multiplexed targeting of dCas9-Spo11 induced a 3.1-, 2.7- and 6.3-fold

increase of crossover frequencies, respectively. The negative controls (expression of the gRNA handle or a gRNA directed against the non-matching *SWC3* gene sequence) show no crossover stimulation above wild type. To note, as DSBs, the crossover frequency was also stimulated at the *PUT4* region by Gal4- and dCas9-Spo11 (3- and 4-fold, respectively) upon deletion of the *GAL4* gene. In the *MSC1* region targeted by QQR-Spo11, recombination is enhanced 5.6-fold over the background and is dependent on the presence of the RS motif. In contrast, no significant stimulation of recombination was observed with the targeting of dCas9-Spo11, consistent with the low increase of targeted DSBs compared to QQR-Spo11 DSBs. Taken together, these results show that like Gal4BD-Spo11 (21,25), the targeting of Spo11 with different types of DNA binding modules increases the meiotic recombination frequency.

DISCUSSION

The data reported here demonstrate that increases in meiotic double-strand breaks and crossover frequencies can be programmed to arbitrary genomic sites in yeast, by fusion of the Spo11 protein to various DNA-recognition domains. These domains include full-length natural transcription factors, synthetic arrays of zinc finger or TALE modules, and

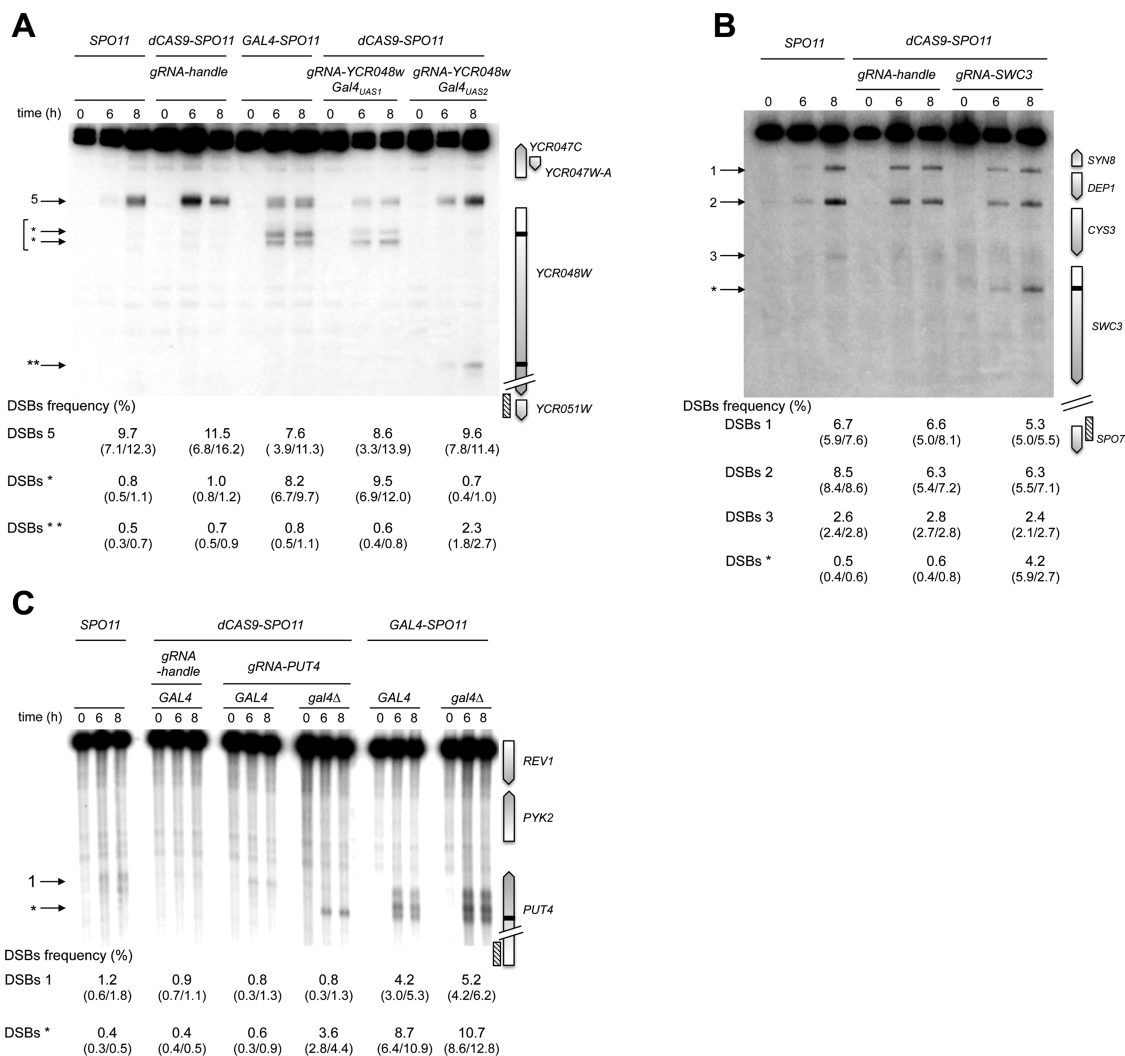


Figure 6. Spo11 fusion DSB formation in targeted gene coding sequences. Southern blot analysis of Gal4-Spo11 and dCas9-Spo11 DSB formation at the target *YCR048W* (A), *SWC3* (B) and *PUT4* (C) ORFs. Gal4-Spo11 and dCas9-Spo11 target sites are shown as black bars at the right of the gel and arrowheads indicate wild-type (numbered) and targeted DSBs (asterisks) at the left of the gel. DSB values as described in Figure 3 legends.

the dCas9 protein in conjunction with designed gRNAs. Importantly, all these Spo11 fusions retain the capacity to form DSBs at the natural sites, thereby ensuring wild-type spore viability, even in the absence of the wild-type *SPO11* gene. At the same time, inactivation of *SPO11* is not necessary for the effect to be manifested (Supplementary Figure S10).

The degree of stimulation of DSB frequencies by the Spo11 fusions was quite variable, depending on the constructs and target sites. Consistently, in most of the cases the crossover frequencies at the successfully targeted loci increased (2.3- to 6.3-fold), with no adverse effect on spore viability (Table 1). In the case of dCas9-Spo11, some of the variability may be due to the quality of the gRNAs, which was not independently tested. Altogether, using Spo11 fusions, we assayed 34 target sites located in 26 different regions (summarized in Table S5) and found that the targeting efficiency varies from site to site, differs according to the TSFs and is modulated by endogenous competition and meiosis-specific binding to the chromatin (Figure 5). Hierarchically, DSB-cold promoter-containing re-

gions are the most efficiently TSF-targeted regions (15/16 cases), suggesting that these ‘permissive’ regions are prone to be warmed-up by the Spo11 fusions. Like the natural DSB hotspots, these TSF-targeted DSBs had a low level of nucleosome occupancy (5), consistent with an open chromatin structure which promotes DNA target accessibility to Spo11 (57–59). Targeting of ORF regions was less successful (6/12 cases) and was located in the proximity of a weak (*PUT4*) or strong DSB hotspot (*YCR048W* and *SWC3*) region. The regional overlap with natural DSB sites likely provides favourable chromatin structure for Spo11 accessibility and cleavage. However, and as previously noted for natural hotspots (5), low nucleosome occupancy is not sufficient to warm up a cold region since TSF-targeting of *GAL2* and *SWC3* gene terminators was inefficient despite a low level of nucleosome occupancy. In agreement with previous results (26), TSFs inefficiently target regions near the centromeres and telomeres where natural DSBs are suppressed, perhaps to ensure proper homolog and sister chromatin segregation. Along this line, our data also show that in many cases, in-

Table 2. The Spo11 fusions stimulate meiotic recombination in the targeted regions

Genotype	Locus	Target site(s)	Targeted DSB frequency (%)	Recombination rate (cM/kb)	Stimulation versus WT
<i>SPO11</i> ^{+/+}	<i>GAL2</i>	—	0.8	0.5	—
<i>GAL4BD-SPO11</i> ^{+/+} ^a	<i>GAL2</i>	<i>ABCD/E</i>	21.1	2.6	5.4
<i>GAL4-SPO11</i> ^{+/+}	<i>GAL2</i>	<i>ABCD/E</i>	21.3	2.5	5.0
<i>TALE-SPO11</i> ^{+/+} <i>gal4Δ</i> ^{+/+}	<i>GAL2</i>	<i>D/E</i>	10.0	1.5	3.1
<i>dCAS9-SPO11</i> ^{-/-} +gRNA handle	<i>GAL2</i>	—	< 0.3	0.6	1.2*
<i>dCAS9-SPO11</i> ^{-/-} +gRNA- <i>SWC3</i>	<i>GAL2</i>	—	< 0.3	0.5	1.0*
<i>dCAS9-SPO11</i> ^{-/-} +gRNA- <i>UAS-D/E</i>	<i>GAL2</i>	<i>D/E</i>	5.4	1.3	2.7
<i>dCAS9-SPO11</i> ^{-/-} + gRNAs- <i>UAS-A, -B, -D/E</i>	<i>GAL2</i>	<i>ABD/E</i>	6.9	3.1	6.3
<i>SPO11</i> ^{+/+}	<i>PUT4</i>	—	1.6	0.9	—
<i>GAL4-SPO11</i> ^{+/+}	<i>PUT4</i>	<i>RS</i>	12.9	2.2	2.3
<i>SPO11</i> ^{+/+} <i>gal4Δ</i> ^{+/+}	<i>PUT4</i>	<i>RS</i>	1.6	0.9	1.0*
<i>GAL4-SPO11</i> ^{+/+} <i>gal4Δ</i> ^{+/+}	<i>PUT4</i>	<i>RS</i>	15.9	2.9	3.2
<i>dCAS9-SPO11</i> ^{-/-} + gRNA handle <i>gal4Δ</i> ^{+/+}	<i>PUT4</i>	<i>RS</i>	1.3	1.8	1.9*
<i>dCAS9-SPO11</i> ^{-/-} + gRNA- <i>UAS gal4Δ</i> ^{+/+}	<i>PUT4</i>	<i>RS</i>	4.4	3.7	4.0
<i>SPO11</i> ^{+/+}	<i>MSG5</i>	—	1.6	0.1	—
<i>TEC1-SPO11</i> ^{+/+}	<i>MSG5</i>	<i>RS</i>	5.2	0.6	4.6
<i>SPO11</i> ^{+/+}	<i>HHF2</i>	—	0.8	0.1	—
<i>RSC3-SPO11</i> ^{+/+}	<i>HHF2</i>	<i>RS</i>	4.6	0.6	6.3
<i>SPO11</i> ^{+/+}	<i>MSC1</i>	—	2.2	0.3	—
<i>QQR-SPO11</i> ^{+/+}	<i>MSC1</i>	<i>RS</i>	23.4	1.7	5.6
<i>QQR-SPO11</i> ^{+/+}	<i>MSC1</i>	<i>rs</i>	4.0	0.2	0.6*
<i>dCAS9-SPO11</i> ^{-/-} +gRNA handle	<i>MSC1</i>	<i>RS</i>	1.4	0.2	0.7*
<i>dCAS9-SPO11</i> ^{-/-} +gRNA- <i>MSC1prom</i>	<i>MSC1</i>	<i>RS</i>	4.5	0.3	1.0*

Recombination rates were measured by introduction of heterozygous genetic markers on either side of the targeted regions and their segregation examined in meiotic products upon tetrad dissection. According to the phenotype of drug resistance, the numbers of parental ditype (PD), tetratype (T) and non-parental ditype (NPD) were determined to calculate the genetic distance in centimorgans (cM) (see Supplementary Table S4 for the complete data). The difference in recombination frequency between the wild-type and TSF strains is statistically different (P -values < 0.05; two-tailed Fisher's exact test), except for those indicated by an asterisk (P -values > 0.2; two-tailed Fisher's exact test).

^aData from (25).

cluding pericentric regions, TSF binding to target site is not sufficient to trigger DSB formation, indicating that other essential *cis* and/or *trans* factor(s) locally regulate cleavage by Spo11 (5,26). For instance, it has been shown that the Cft19 complex inhibits DSB formation near the centromere (54). Thus so far, some genomic sites still remain refractory to DSB targeting and their warming will require further innovations.

Another factor that influences the ability to program DSBs with Spo11 fusions is occupancy of the target by endogenous DNA-binding proteins. The level of stimulation at natural Gal4 binding sites by Gal4-, TALE- and dCas9-Spo11 was enhanced by deletion of the endogenous *GAL4* gene. This effect was less pronounced for Gal4-Spo11, suggesting either that it has a higher inherent affinity for its target sequence, or that it is better able to compete with the endogenous protein. This advantage may apply to other natural transcription factors as well; however, not all apparent binding sites for these proteins can be accessed. For example, only about 25 of the identified 496 Gal4_{UAS} sites in the yeast SK1 genome are bound *in vivo* (26,60).

Since all TSFs were expressed under the same promoter and since the amount of TSF activity does not seem to be limiting (Table 1), a comparison of targeted recombination efficiency between the various Spo11 fusions is possible. This is summarized in Table 2. In the targeted *GAL2* promoter and *PUT4* gene, Gal4- and CRISPR-dCas9-Spo11 constructs induce similar level of recombination stimulation (5.0 versus 6.3 and 3.2 versus 4.0-fold, respectively and not statistically different). The fact that Gal4 binds to > 25 targets genome-wide (26,60) instead of up to three for

CRISPR-dCas9 and that CRISPR-dCas9 is much more sensitive to native Gal4 target-binding competition, suggests that Gal4 has a stronger affinity for the Gal4_{UAS} sites *in vivo* than the CRISPR-dCas9 system. Similarly, TALE- and CRISPR-dCas9-Spo11 lead to an approximately 3-fold enhancement of recombination frequency in the *GAL2* region containing the unique target Gal4_{UASD/E} site but TALE-Spo11 efficiency is strongly impaired by endogenous Gal4 interference. It suggests that CRISPR-dCas9 displays a higher affinity for the Gal4_{UASD/E} site than TALE. In contrast, CRISPR-dCas9-Spo11 poorly stimulates DSBs at the *MSC1* promoter while QQR-Spo11 is very proficient and enhanced approximately 6-fold the targeted crossover frequency. It suggests that QQR has a tighter binding capacity to this target site than CRISPR-dCas9-Spo11, being driven by a proficient DNA binding affinity and/or being assisted by other protein-protein chromatin interactions. Thus, choosing endogenous transcription factors from the host organism may sometimes be more efficient as transcription factors are likely evolutionarily selected proteins most able to find their target and overcome competition with other native factors. Although there are little comparative data, zinc fingers and TALE nucleases seem to be just as effective (and sometimes more effective) for particular target site than the CRISPR system, indicating again that the efficiency of the programmable Spo11 fusions can vary greatly among targets.

The disadvantage to natural factors is that they do not allow programming to arbitrary regions of the genome. In contrast, zinc fingers, TALE domains and the CRISPR-Cas9 platform can all be directed to a wide range of se-

quences. It is worth noting that the different programmable Spo11 fusions generate DSBs with varying degrees of efficiency at the same target locus (Figures 3 and 4D and Supplementary Figure S3B). However, dCas9-Spo11 has several advantages: design for new targets is very simple (just production of new gRNAs) and a desired target region can be investigated by testing a number of different gRNAs. Multiple gRNAs can be introduced together, and this can improve DSB formation above any single gRNA (see Figure 3B).

An alternative approach to stimulating recombination frequencies is to manipulate the processing of meiotic DSBs at the repair stages. Previous studies in *A. thaliana* demonstrated that stimulation of meiotic crossovers is obtained in mutant lines that alter the outcome of a subset of DSB repair events (27–30). In this case, elevated rates were only observed at natural crossover sites, along the non-interfering CO pathway. In contrast, the Spo11 fusions described here allow to modify recombination initiation and produce experimental alteration of the location and frequencies of DSBs, with the consequence to locally enhance gene conversion and crossover frequencies (21,25) (present data).

Modifying the natural meiotic recombination landscape is a highly desirable biotechnological advance. Overcoming the generally low level of recombination events per chromosome per generation (1 or 2) observed in most eukaryotes will facilitate the separation or re-association of closely-linked alleles in hybrid strains. This promises to significantly reduce the cost and timeframe for the development, for example, of novel plant varieties.

SUPPLEMENTARY DATA

Supplementary Data are available at NAR Online.

ACKNOWLEDGEMENTS

We are grateful to all members of our laboratory, especially to L. Carrière and S. Loeillet for many fruitful discussions.

FUNDING

ANR [BLAN06-3-150811]; ARC and MeioGenix©; CNRS and the Institut Curie (to N.U.). Funding for open access charge: Institut Curie.

Conflict of interest statement. A.N. and G.B. are CSO and CEO, cofounders of MeioGenix, respectively. G.B. and A.S. are employed by MeioGenix. G.B., A.N. and A.S. are inventors of a patent issued from this research.

REFERENCES

- Nagaoka, S.I., Hassold, T.J. and Hunt, P.A. (2012) Human aneuploidy: mechanisms and new insights into an age-old problem. *Nat. Rev. Genet.*, **13**, 493–504.
- Bergerat, A., de Massy, B., Gabelle, D., Varoutas, P.C., Nicolas, A. and Forterre, P. (1997) An atypical topoisomerase II from Archaea with implications for meiotic recombination. *Nature*, **386**, 414–417.
- Keeney, S., Giroux, C.N. and Kleckner, N. (1997) Meiosis-specific DNA double-strand breaks are catalyzed by Spo11, a member of a widely conserved protein family. *Cell*, **88**, 375–384.
- Keeney, S. (2007) Spo11 and the Formation of DNA Double-strand Breaks in Meiosis. In: Lankenau, D.H. (ed). *Genome dynamics and stability*. Springer-Verlag, Heidelberg, pp. 81–123.
- Pan, J., Sasaki, M., Kniewel, R., Murakami, H., Blitzblau, H.G., Tischfield, S.E., Zhu, X., Neale, M.J., Jasin, M., Socci, N.D. *et al.* (2011) A hierarchical combination of factors shapes the genome-wide topography of yeast meiotic recombination initiation. *Cell*, **144**, 719–731.
- Mancera, E., Bourgon, R., Brozzi, A., Huber, W. and Steinmetz, L.M. (2008) High-resolution mapping of meiotic crossovers and non-crossovers in yeast. *Nature*, **454**, 479–485.
- Choi, K., Zhao, X., Kelly, K.A., Venn, O., Higgins, J.D., Yelina, N.E., Hardcastle, T.J., Ziolkowski, P.A., Copenhagen, G.P., Franklin, F.C. *et al.* (2013) Arabidopsis meiotic crossover hot spots overlap with H2A.Z nucleosomes at gene promoters. *Nat. Genet.*, **45**, 1327–1336.
- Holloway, J.K., Booth, J., Edelmann, W., McGowan, C.H. and Cohen, P.E. (2008) MUS81 generates a subset of MLH1-MLH3-independent crossovers in mammalian meiosis. *PLoS Genet.*, **4**, e1000186.
- Martini, E., Diaz, R.L., Hunter, N. and Keeney, S. (2006) Crossover homeostasis in yeast meiosis. *Cell*, **126**, 285–295.
- Lam, I. and Keeney, S. (2014) Mechanism and regulation of meiotic recombination initiation. *Cold Spring Harb. Perspect. Biol.*, **7**, a016634.
- Keeney, S., Lange, J. and Mohibullah, N. (2014) Self-organization of meiotic recombination initiation: general principles and molecular pathways. *Annu. Rev. Genet.*, **48**, 187–214.
- Nadarajan, S., Lambert, T.J., Altendorfer, E., Gao, J., Blower, M.D., Waters, J.C. and Colaiacovo, M.P. (2017) Polo-like kinase-dependent phosphorylation of the synaptonemal complex protein SYP-4 regulates double-strand break formation through a negative feedback loop. *Elife*, **6**, e23437.
- Higgins, J.D., Osman, K., Jones, G.H. and Franklin, F.C. (2014) Factors underlying restricted crossover localization in barley meiosis. *Annu. Rev. Genet.*, **48**, 29–47.
- Choulet, F., Alberti, A., Theil, S., Glover, N., Barbe, V., Daron, J., Pingault, L., Sourdil, P., Couloux, A., Paux, E. *et al.* (2014) Structural and functional partitioning of bread wheat chromosome 3B. *Science*, **345**, 1249721.
- Borde, V. and de Massy, B. (2013) Programmed induction of DNA double strand breaks during meiosis: setting up communication between DNA and the chromosome structure. *Curr. Opin. Genet. Dev.*, **23**, 147–155.
- de Massy, B. (2013) Initiation of meiotic recombination: how and where? Conservation and specificities among eukaryotes. *Annu. Rev. Genet.*, **47**, 563–599.
- Mercier, R., Mezard, C., Jenczewski, E., Macaisne, N. and Grelon, M. (2015) The molecular biology of meiosis in plants. *Annu. Rev. Plant Biol.*, **66**, 297–327.
- Lam, I. and Keeney, S. (2015) Nonparadoxical evolutionary stability of the recombination initiation landscape in yeast. *Science*, **350**, 932–937.
- Lesecque, Y., Glemin, S., Lartillot, N., Mouchiroud, D. and Duret, L. (2014) The red queen model of recombination hotspots evolution in the light of archaic and modern human genomes. *PLoS Genet.*, **10**, e1004790.
- Singhal, S., Leffler, E.M., Sannareddy, K., Turner, I., Venn, O., Hooper, D.M., Strand, A.I., Li, Q., Raney, B., Balakrishnan, C.N. *et al.* (2015) Stable recombination hotspots in birds. *Science*, **350**, 928–932.
- Pecina, A., Smith, K.N., Mezard, C., Murakami, H., Ohta, K. and Nicolas, A. (2002) Targeted stimulation of meiotic recombination. *Cell*, **111**, 173–184.
- Nicolas, A. (2009) Modulating and targeting meiotic double-strand breaks in *Saccharomyces cerevisiae*. *Methods Mol. Biol.*, **557**, 27–33.
- Smagulova, F., Brick, K., Pu, Y., Sengupta, U., Camerini-Otero, R.D. and Petukhova, G.V. (2013) Suppression of genetic recombination in the pseudoautosomal region and at subtelomeres in mice with a hypomorphic Spo11 allele. *BMC Genomics*, **14**, 493.
- Szekvolgyi, L., Ohta, K. and Nicolas, A. (2015) Initiation of meiotic homologous recombination: flexibility, impact of histone modifications, and chromatin remodeling. *Cold Spring Harb. Perspect. Biol.*, **7**, a016527.
- Murakami, H. and Nicolas, A. (2009) Locally, meiotic double-strand breaks targeted by Gal4BD-Spo11 occur at discrete sites with a sequence preference. *Mol. Cell Biol.*, **29**, 3500–3516.
- Robine, N., Uematsu, N., Amiot, F., Gidrol, X., Barillot, E., Nicolas, A. and Borde, V. (2007) Genome-wide redistribution of meiotic

- double-strand breaks in *Saccharomyces cerevisiae*. *Mol. Cell Biol.*, **27**, 1868–1880.
27. Crismani, W., Girard, C., Froger, N., Pradillo, M., Santos, J.L., Chelysheva, L., Copenhaver, G.P., Horlow, C. and Mercier, R. (2012) FANCM limits meiotic crossovers. *Science*, **336**, 1588–1590.
 28. Girard, C., Chelysheva, L., Choinard, S., Froger, N., Macaisne, N., Lemhemdi, A., Mazel, J., Crismani, W. and Mercier, R. (2015) AAA-ATPase FIDGETIN-LIKE 1 and helicase FANCM antagonize meiotic crossovers by distinct mechanisms. *PLoS Genet.*, **11**, e1005369.
 29. Seguela-Arnaud, M., Crismani, W., Larcheveque, C., Mazel, J., Froger, N., Choinard, S., Lemhemdi, A., Macaisne, N., Van Leene, J., Gevaert, K. *et al.* (2015) Multiple mechanisms limit meiotic crossovers: TOP3alpha and two BLM homologs antagonize crossovers in parallel to FANCM. *Proc. Natl. Acad. Sci. U.S.A.*, **112**, 4713–4718.
 30. Ziolkowski, P.A., Underwood, C.J., Lambing, C., Martinez-Garcia, M., Lawrence, E.J., Ziolkowska, L., Griffin, C., Choi, K., Franklin, F.C., Martienssen, R.A. *et al.* (2017) Natural variation and dosage of the HEI10 meiotic E3 ligase control Arabidopsis crossover recombination. *Genes Dev.*, **31**, 306–317.
 31. Smith, J., Bibikova, M., Whitby, F.G., Reddy, A.R., Chandrasegaran, S. and Carroll, D. (2000) Requirements for double-strand cleavage by chimeric restriction enzymes with zinc finger DNA-recognition domains. *Nucleic Acids Res.*, **28**, 3361–3369.
 32. Jinek, M., Chylinski, K., Fonfara, I., Hauer, M., Doudna, J.A. and Charpentier, E. (2012) A programmable dual-RNA-guided DNA endonuclease in adaptive bacterial immunity. *Science*, **337**, 816–821.
 33. Cong, L., Ran, F.A., Cox, D., Lin, S., Barretto, R., Habib, N., Hsu, P.D., Wu, X., Jiang, W., Marraffini, L.A. *et al.* (2013) Multiplex genome engineering using CRISPR/Cas systems. *Science*, **339**, 819–823.
 34. Farzadfard, F., Perli, S.D. and Lu, T.K. (2013) Tunable and multifunctional eukaryotic transcription factors based on CRISPR/Cas. *ACS Synthetic Biol.*, **2**, 604–613.
 35. Kane, S.M. and Roth, R. (1974) Carbohydrate metabolism during ascospore development in yeast. *J. Bacteriol.*, **118**, 8–14.
 36. Goldstein, A.L. and McCusker, J.H. (1999) Three new dominant drug resistance cassettes for gene disruption in *Saccharomyces cerevisiae*. *Yeast*, **15**, 1541–1553.
 37. Borde, V., Robine, N., Lin, W., Bonfils, S., Geli, V. and Nicolas, A. (2009) Histone H3 lysine 4 trimethylation marks meiotic recombination initiation sites. *EMBO J.*, **28**, 99–111.
 38. Sasanuma, H., Murakami, H., Fukuda, T., Shibata, T., Nicolas, A. and Ohta, K. (2007) Meiotic association between Spo11 regulated by Rec102, Rec104 and Rec114. *Nucleic Acids Res.*, **35**, 1119–1133.
 39. Murakami, H., Borde, V., Nicolas, A. and Keeney, S. (2009) Gel electrophoresis assays for analyzing DNA double-strand breaks in *Saccharomyces cerevisiae* at various spatial resolutions. *Methods Mol. Biol.*, **557**, 117–142.
 40. Jiang, F., Zhou, K., Ma, L., Gressel, S. and Doudna, J.A. (2015) A Cas9-guide RNA complex preorganized for target DNA recognition. *Science*, **348**, 1477–1481.
 41. Bibikova, M., Carroll, D., Segal, D.J., Trautman, J.K., Smith, J., Kim, Y.G. and Chandrasegaran, S. (2001) Stimulation of homologous recombination through targeted cleavage by chimeric nucleases. *Mol. Cell Biol.*, **21**, 289–297.
 42. Boch, J., Scholze, H., Schornack, S., Landgraf, A., Hahn, S., Kay, S., Lahaye, T., Nickstadt, A. and Bonas, U. (2009) Breaking the code of DNA binding specificity of TAL-type III effectors. *Science*, **326**, 1509–1512.
 43. Bogdanove, A.J. and Voytas, D.F. (2011) TAL effectors: customizable proteins for DNA targeting. *Science*, **333**, 1843–1846.
 44. Zenvirth, D., Arbel, T., Sherman, A., Goldway, M., Klein, S. and Simchen, G. (1992) Multiple sites for double-strand breaks in whole meiotic chromosomes of *Saccharomyces cerevisiae*. *EMBO J.*, **11**, 3441–3447.
 45. Baudat, F. and Nicolas, A. (1997) Clustering of meiotic double-strand breaks on yeast chromosome III. *Proc. Natl. Acad. Sci. U.S.A.*, **94**, 5213–5218.
 46. Parthun, M.R. and Jaehning, J.A. (1990) Purification and characterization of the yeast transcriptional activator GAL4. *J. Biol. Chem.*, **265**, 209–213.
 47. Vashee, S., Xu, H., Johnston, S.A. and Kodadek, T. (1993) How do ‘Zn2 cys6’ proteins distinguish between similar upstream activation sites? Comparison of the DNA-binding specificity of the GAL4 protein in vitro and in vivo. *J. Biol. Chem.*, **268**, 24699–24706.
 48. Koehn, D.R., Haring, S.J., Williams, J.M. and Malone, R.E. (2009) Tethering recombination initiation proteins in *Saccharomyces cerevisiae* promotes double strand break formation. *Genetics*, **182**, 447–458.
 49. Vedel, M. and Nicolas, A. (1999) CYS3, a hotspot of meiotic recombination in *Saccharomyces cerevisiae*. Effects of heterozygosity and mismatch repair functions on gene conversion and recombination intermediates. *Genetics*, **151**, 1245–1259.
 50. Buhler, C., Borde, V. and Lichten, M. (2007) Mapping meiotic single-strand DNA reveals a new landscape of DNA double-strand breaks in *Saccharomyces cerevisiae*. *PLoS Biol.*, **5**, e324.
 51. Si, W., Yuan, Y., Huang, J., Zhang, X., Zhang, Y., Zhang, Y., Tian, D., Wang, C., Yang, Y. and Yang, S. (2015) Widely distributed hot and cold spots in meiotic recombination as shown by the sequencing of rice F2 plants. *New Phytol.*, **206**, 1491–1502.
 52. Goshima, G. and Yanagida, M. (2000) Establishing biorientation occurs with precocious separation of the sister kinetochores, but not the arms, in the early spindle of budding yeast. *Cell*, **100**, 619–633.
 53. Blitzblau, H.G., Bell, G.W., Rodriguez, J., Bell, S.P. and Hochwagen, A. (2007) Mapping of meiotic single-stranded DNA reveals double-stranded-break hotspots near centromeres and telomeres. *Curr. Biol.*, **17**, 2003–2012.
 54. Vincenten, N., Kuhl, L.M., Lam, I., Oke, A., Kerr, A.R., Hochwagen, A., Fung, J., Keeney, S., Vader, G. and Marston, A.L. (2015) The kinetochore prevents centromere-proximal crossover recombination during meiosis. *Elife*, **4**, e10850.
 55. Lange, J., Yamada, S., Tischfield, S.E., Pan, J., Kim, S., Zhu, X., Succi, N.D., Jasin, M. and Keeney, S. (2016) The landscape of mouse meiotic double-strand break formation, processing, and repair. *Cell*, **167**, 695–708.
 56. Sasaki, M., Tischfield, S.E., van Overbeek, M. and Keeney, S. (2013) Meiotic recombination initiation in and around retrotransposable elements in *Saccharomyces cerevisiae*. *PLoS Genet.*, **9**, e1003732.
 57. Ohta, K., Shibata, T. and Nicolas, A. (1994) Changes in chromatin structure at recombination initiation sites during yeast meiosis. *EMBO J.*, **13**, 5754–5763.
 58. Wu, T.C. and Lichten, M. (1994) Meiosis-induced double-strand break sites determined by yeast chromatin structure. *Science*, **263**, 515–518.
 59. Lichten, M. (2008) Meiotic Chromatin: The Substrate for Recombination Initiation. In: Lankenau, D.H. (ed). *Recombination and Meiosis*. Springer-Verlag, Heidelberg, pp. 165–196.
 60. Ren, B., Robert, F., Wyrick, J.J., Aparicio, O., Jennings, E.G., Simon, I., Zeitlinger, J., Schreiber, J., Hannett, N., Kanin, E. *et al.* (2000) Genome-wide location and function of DNA binding proteins. *Science*, **290**, 2306–2309.